

The nuclear matter density functional under the nucleonic hypothesis

Hoa Dinh Thi, Chiranjib Mondal, Francesca Gulminelli

Journées de Rencontre des Jeunes Chercheurs 2021

17-23 October, 2021

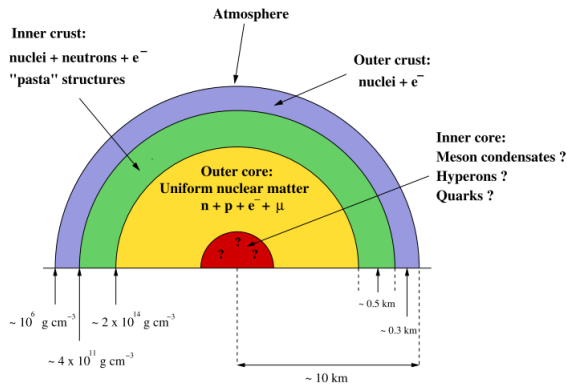


Neutron Stars

- $M \sim 1 - 2 M_{\odot}$

- $R \sim 10 - 15 \text{ km}$

→ Contain matter under **extreme** conditions.



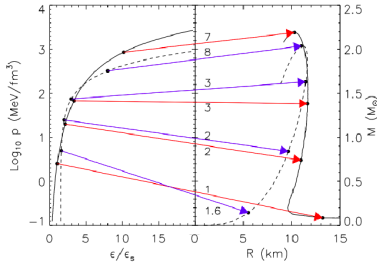
Fiorella Burgio, G.; Vidaña, I. Universe 2020, 6(8), 119

Tolman-Oppenheimer-Volkoff (TOV) equation

Hydrostatic equilibrium equations:

$$\frac{dP}{dr} = -\frac{G\rho m}{r^2} \left(1 + \frac{P}{\rho c^2}\right) \left(1 + \frac{4\pi P r^3}{mc^2}\right) \left(1 - \frac{2Gm}{c^2 r}\right)^{-1},$$
$$\frac{dm}{dr} = 4\pi r^2 \rho,$$

→ Needs an **equation of state (EoS)**, $P = P(\rho)$, to complete the system of equations.



Motivations

- The EoS around saturation density is well-constrained by **nuclear physics** experiments and theory, while the EoS behavior at high densities remains a challenge.

Motivations

- The EoS around saturation density is well-constrained by **nuclear physics** experiments and theory, while the EoS behavior at high densities remains a challenge.
- The first direct detection of gravitational waves from the merger of a binary NS system on 17 August 2017 (**GW170817**) by **LVC** opens great opportunities to understand better the dense-matter EoS.

Motivations

- The EoS around saturation density is well-constrained by **nuclear physics** experiments and theory, while the EoS behavior at high densities remains a challenge.
- The first direct detection of gravitational waves from the merger of a binary NS system on 17 August 2017 (**GW170817**) by **LVC** opens great opportunities to understand better the dense-matter EoS.
- Very recently, the **radius** of massive pulsar PSR J0740+6620 is measured with **NICER and XMM Newton** data.

Motivations

- The EoS around saturation density is well-constrained by **nuclear physics** experiments and theory, while the EoS behavior at high densities remains a challenge.
- The first direct detection of gravitational waves from the merger of a binary NS system on 17 August 2017 (**GW170817**) by **LVC** opens great opportunities to understand better the dense-matter EoS.
- Very recently, the **radius** of massive pulsar PSR J0740+6620 is measured with **NICER** and **XMM Newton** data.
→ This work aims to study the combined implications of these measurements on the **nucleonic EoS** using **meta-modeling** techniques by performing **Bayesian analysis**.

Meta-modeling of the EoS

* Nuclear matter energy per nucleon ($n = n_p + n_n$, $\delta = (n_n - n_p)/n$):

$$e(n, \delta) = e_{is}(n) + \delta^2 e_{iv}(n)$$

Meta-modeling of the EoS

* Nuclear matter energy per nucleon ($n = n_p + n_n$, $\delta = (n_n - n_p)/n$):

$$e(n, \delta) = e_{is}(n) + \delta^2 e_{iv}(n)$$

* Taylor expansions ($x = \frac{n-n_{sat}}{3n_{sat}}$):

$$e_{is} = E_{sat} + \frac{1}{2} K_{sat} x^2 + \frac{1}{3!} Q_{sat} x^3 + \frac{1}{4!} Z_{sat} x^4 + \dots$$

$$e_{iv} = E_{sym} + L_{sym} x + \frac{1}{2} K_{sym} x^2 + \frac{1}{3!} Q_{sym} x^3 + \frac{1}{4!} Z_{sym} x^4 + \dots$$

Meta-modeling of the EoS

- * Nuclear matter energy per nucleon ($n = n_p + n_n$, $\delta = (n_n - n_p)/n$):

$$e(n, \delta) = e_{is}(n) + \delta^2 e_{iv}(n)$$

- * Taylor expansions ($x = \frac{n-n_{sat}}{3n_{sat}}$):

$$e_{is} = E_{sat} + \frac{1}{2} K_{sat} x^2 + \frac{1}{3!} Q_{sat} x^3 + \frac{1}{4!} Z_{sat} x^4 + \dots$$

$$e_{iv} = E_{sym} + L_{sym} x + \frac{1}{2} K_{sym} x^2 + \frac{1}{3!} Q_{sym} x^3 + \frac{1}{4!} Z_{sym} x^4 + \dots$$

- * In meta-modeling:

$$e(n, \delta) = t_{FG}(n, \delta) + v(n, \delta).$$

See Margueron et al. Phys. Rev. C 2018, 97:025806

Why meta-modeling?

- All purely nucleonic models can be nicely reproduced with the metamodel by truncating the expansion at order 4.

Why meta-modeling?

- All purely nucleonic models can be nicely reproduced with the metamodel by truncating the expansion at order 4.
- No correlation is assumed *a priori* among the empirical parameters.

Why meta-modeling?

- All purely nucleonic models can be nicely reproduced with the metamodel by truncating the expansion at order 4.
- No correlation is assumed *a priori* among the empirical parameters.
- Metamodel, complemented by surface and curvature parameters ($\{\sigma_0, b_s, \sigma_{0c}, \beta\}$) in CLDM, allows making a unified treatment of the crust.

Why meta-modeling?

- All purely nucleonic models can be nicely reproduced with the metamodel by truncating the expansion at order 4.
- No correlation is assumed *a priori* among the empirical parameters.
- Metamodel, complemented by surface and curvature parameters ($\{\sigma_0, b_s, \sigma_{0c}, \beta\}$) in CLDM, allows making a unified treatment of the crust.

→ Deviations between observations and metamodel predictions will signal the failure of the nucleonic approximation, and therefore reveal the presence of deconfined matter at high density.

Bayesian analysis

Posterior

$$P(\{X\}|c) = \mathcal{N} P_{prior}(\{X\}) \prod_k P(c_k|\{X\})$$

Bayesian analysis

Posterior

$$P(\{X\}|c) = \mathcal{N} P_{prior}(\{X\}) \prod_k P(c_k|X)$$

Prior

- Bulk parameters $\{X\}$:

Parameters	Min	Max
E_{sat} (MeV)	-17	-15
n_{sat} (fm^{-3})	0.15	0.17
K_{sat} (MeV)	190	270
Q_{sat} (MeV)	-1000	1000
Z_{sat} (MeV)	-3000	3000
E_{sym} (MeV)	26	38
L_{sym} (MeV)	10	80
K_{sym} (MeV)	-400	200
Q_{sym} (MeV)	-2000	2000
Z_{sym} (MeV)	-5000	5000
m_{sat}^*	0.6	0.8
$\Delta m_{sat}^*/m$	0.0	0.2
b	1	10

Margueron et al. Phys. Rev. C 2018,
97:025806

Bayesian analysis

Posterior

$$P(\{X\}|c) = \mathcal{N} P_{prior}(\{X\}) \prod_k P(c_k|X)$$

Prior

- Bulk parameters $\{X\}$:

Parameters	Min	Max
E_{sat} (MeV)	-17	-15
n_{sat} (fm^{-3})	0.15	0.17
K_{sat} (MeV)	190	270
Q_{sat} (MeV)	-1000	1000
Z_{sat} (MeV)	-3000	3000
E_{sym} (MeV)	26	38
L_{sym} (MeV)	10	80
K_{sym} (MeV)	-400	200
Q_{sym} (MeV)	-2000	2000
Z_{sym} (MeV)	-5000	5000
m_{sat}^*	0.6	0.8
$\Delta m_{sat}^*/m$	0.0	0.2
b	1	10

- Surface and curvature parameters:

$$\{\sigma_0, b_s, \sigma_{0c}, \beta\}.$$

Fit to AME2016 mass table:

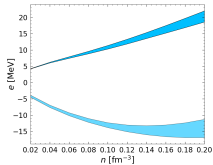
$$p_{AME}(\{X\}) = e^{-\chi^2(\{X\})/2}$$

Huang et al. Chin. Phys. C
2017, 41, 03000

Margueron et al. Phys. Rev. C 2018,
97:025806

Constraints from nuclear physics and astrophysical observations

1. Chiral EFT calculation:

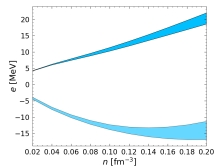


Drischler et al. Phys. Rev. C 2016, 93, 054314.

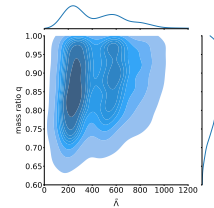
Constraints from nuclear physics and astrophysical observations

2. GW170817 by LVC:

1. Chiral EFT calculation:



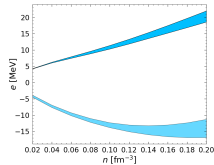
Drischler et al. Phys. Rev. C 2016, 93, 054314.



Abbott et al. Phys. Rev. X 2019, 9(1):011001.

Constraints from nuclear physics and astrophysical observations

1. Chiral EFT calculation:

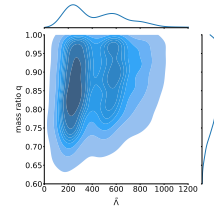


Drischler et al. Phys. Rev. C 2016, 93, 054314.

3. PSR 0348+0432 mass: $M = 2.01 \pm 0.04 M_{\odot}$

Antoniadis et al. Science 2013, 340.

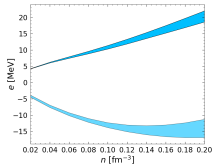
2. GW170817 by LVC:



Abbott et al. Phys. Rev. X 2019, 9(1):011001.

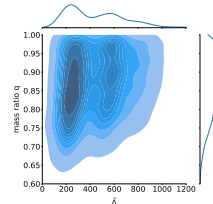
Constraints from nuclear physics and astrophysical observations

1. Chiral EFT calculation:



Drischler et al. Phys. Rev. C 2016, 93, 054314.

2. GW170817 by LVC:

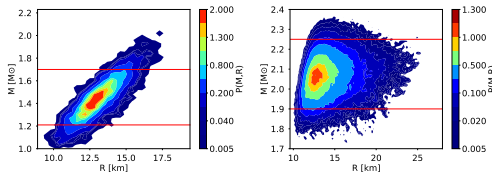


Abbott et al. Phys. Rev. X 2019, 9(1):011001.

3. PSR 0348+0432 mass: $M = 2.01 \pm 0.04 M_{\odot}$

Antoniadis et al. Science 2013, 340.

4. PSR J0030+0451 (NICER, 2019) & J0740+6620 (NICER+XMM, 2021) mass and radius measurement



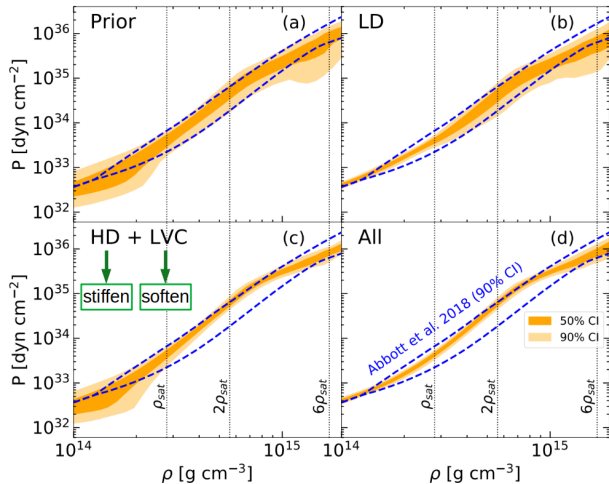
Miller et al. Astrophys. J. Lett. 2019, 887, L24; Miller et al 2021, arXiv:2105.06979

Results

- ① **Prior**
- ② **LD:** EFT calculation
- ③ **HD+LVC:** (causality, stability, $e_{sym} > 0$) + NS mass + LVC
- ④ **All:** EFT calculation + HD + LVC + NICER

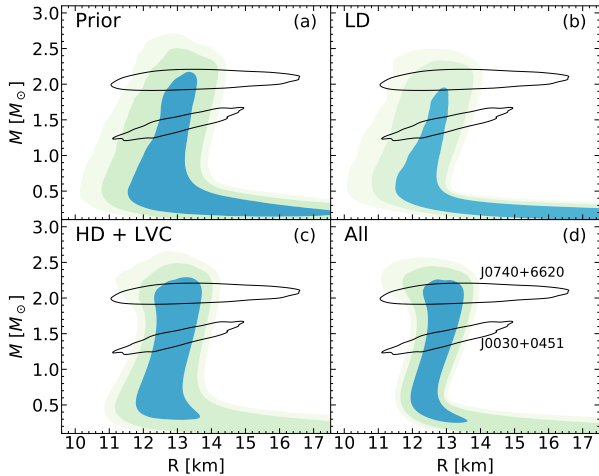
See Dinh Thi, H.; Mondal, C.; Gulminelli, F. Universe 2021, 7, 373.

Equation of State



→ Good agreement with GW170817.

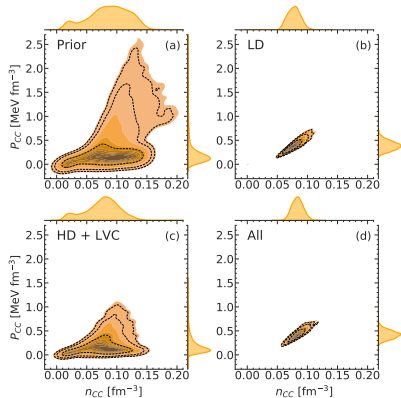
M-R relation



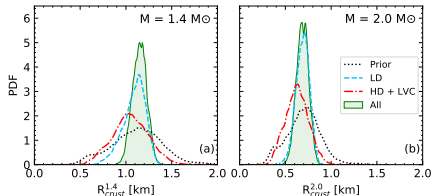
→ Good agreement with NICER measurements.

Crustal properties

Crust-core transition



Crust thickness

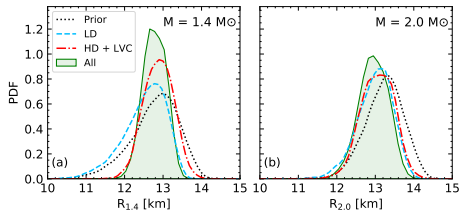


→ Crust properties are mostly constrained by χ EFT calculation.

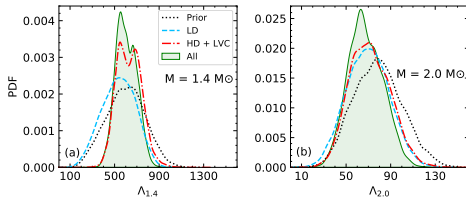
→ $R_{\text{crust}}^{1.4} = 1.15^{+0.10}_{-0.08} \text{ km}$; $R_{\text{crust}}^{2.0} = 0.687^{+0.067}_{-0.067} \text{ km}$.

Radius and Tidal deformability

Radius



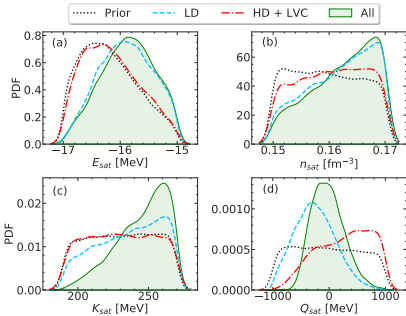
Dim. less tidal deformability



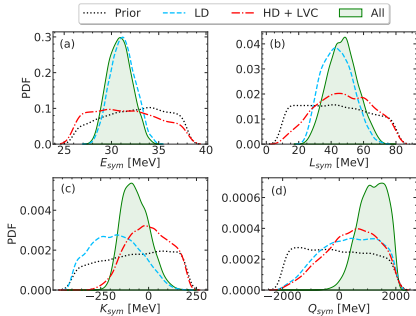
$$R_{1.4} = 12.78^{+0.30}_{-0.29} \text{ km. (Miller et al. 2021: } R_{1.4} = 12.45 \pm 0.65 \text{ km)}$$

Empirical EoS parameters

Isoscalar parameters



Isovector parameters



- χ EFT: most effective in low-order isovector parameters (E_{sym} , L_{sym}).
- Astro: most effective in high-order parameters (Q_{sat} , K_{sym} , Q_{sym}).

Correlation between observables and parameters

	E_{sat}	η_{sat}	K_{sat}	Q_{sat}	Z_{sat}	E_{sym}	L_{sym}	K_{sym}	Q_{sym}	Z_{sym}	σ_0	b_s	σ_{0c}	β
n_{CC}	-0.09	-0.05	0.15	-0.11	0.00	-0.34	-0.69	-0.22	0.55	-0.16	0.10	0.43	-0.17	-0.10
P_{CC}	-0.05	-0.02	0.13	-0.03	-0.03	-0.07	-0.62	-0.38	0.41	-0.04	0.05	0.12	-0.02	-0.05
$R_{crust}^{1.4}$	0.09	-0.18	0.19	0.15	0.09	-0.01	-0.14	0.20	0.64	0.01	-0.09	-0.08	0.04	0.08
$R_{1.4}$	0.15	-0.22	0.13	0.20	0.14	-0.03	0.41	0.65	0.42	0.06	-0.14	-0.12	0.02	0.13
$\Lambda_{1.4}$	0.16	-0.24	0.16	0.23	0.14	-0.17	0.26	0.60	0.50	0.10	-0.15	0.00	-0.01	0.14
$x_p^{1.4}$	-0.24	0.32	-0.41	-0.50	-0.09	0.39	0.60	0.75	0.58	0.04	0.22	-0.15	-0.06	-0.20
$R_{crust}^{2.0}$	0.15	-0.23	0.27	0.31	0.19	-0.16	-0.26	0.08	0.53	0.12	-0.14	0.00	0.05	0.14
$R_{2.0}$	0.21	-0.27	0.24	0.38	0.25	-0.19	0.10	0.36	0.37	0.18	-0.19	-0.01	0.04	0.18
$\Lambda_{2.0}$	0.22	-0.29	0.27	0.42	0.27	-0.28	-0.03	0.27	0.36	0.21	-0.20	0.05	0.03	0.19
$x_p^{2.0}$	-0.20	0.19	-0.39	-0.57	-0.29	0.20	0.31	0.51	0.62	0.25	0.19	-0.00	-0.12	-0.18

Conclusions

- Low-density nuclear physics data constrains the crustal properties, while astrophysical data constrains the global NS properties.

Conclusions

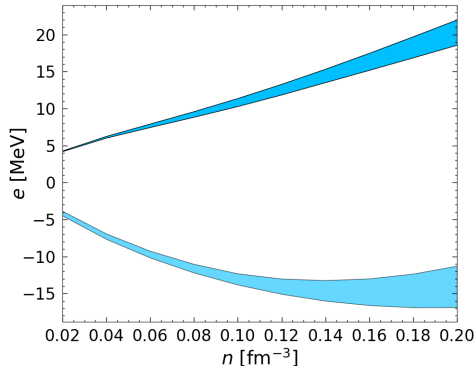
- Low-density nuclear physics data constrains the crustal properties, while astrophysical data constrains the global NS properties.
- The nucleonic hypothesis is consistent with all current data.

Conclusions

- Low-density nuclear physics data constrains the crustal properties, while astrophysical data constrains the global NS properties.
- The nucleonic hypothesis is consistent with all current data.
- We need more stringent constraints from the observations to conclusively establish (reject) the presence of exotic degrees of freedom in high-density matter.

Backup slides 1: Bayesian analysis

1. Chiral EFT calculation:



- Inside the bands:
 $\omega_{EFT} = 1$.
- Outside the bands:
 $\omega_{EFT} = 0$.

Drischler et al, Phys. Rev. C93, 054314 (2016).

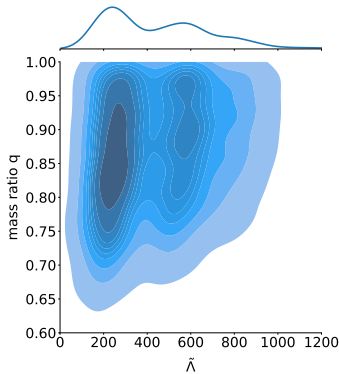
2. PSR 0348+0432 mass measurement, $M = 2.01 \pm 0.04 M_{\odot}$:

$$P(M_{max} | \{X\}) = \int_0^{M_{max}(\{X\})} e^{-\frac{(x-2.01)^2}{2 \times 0.04^2}} dx$$

Antoniadis et al. 2013, Science, 340, 6131

3. GW170817 by LVC:

$$P(LVC|\{X\}) = \sum_i P_{LVC}(\tilde{\Lambda}(q^{(i)}), q^{(i)})$$

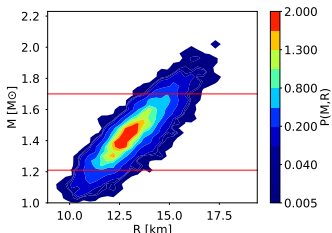


$$\tilde{\Lambda} = \frac{16}{13} \frac{(m_1 + 12m_2)m_1^4\Lambda_1 + (m_2 + 12m_1)m_2^4\Lambda_2}{(m_1 + m_2)^5}$$

- $q \in [0.73, 1.0]$, with step 0.01
 $\rightarrow m_1, m_2$

Abbott et al, Physical Review X, 9(1):011001, 2019.
<https://dcc.ligo.org/LIGO-P1800061/public>

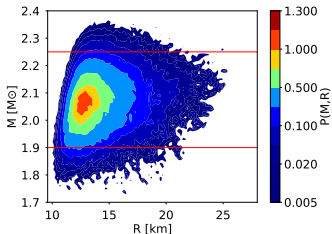
4. Mass and radius measurement of J0030+0451 from NICER data:



$$P(NICER19|\{X\}) = \sum_i p_{NICER1}(M^{(i)}, R(M^{(i)}))$$

$M \in [1.21, 1.70] M_\odot$, step of $0.03 M_\odot$.
→ 17 grid points.

5. Radius measurement of PSR J0740+6620 from NICER-XMM data:



$$P(NICER21|\{X\}) = \sum_i p_{NICER2}(M^{(i)}, R(M^{(i)}))$$

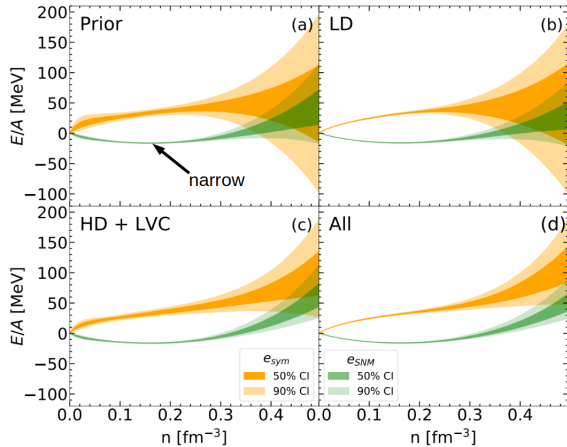
$M \in [1.90, 2.25] M_\odot$, step of $0.01 M_\odot$.
→ 36 grid points.

Miller et al, *Astrophys. 376 J. Lett. 887, L24 (2019)*.

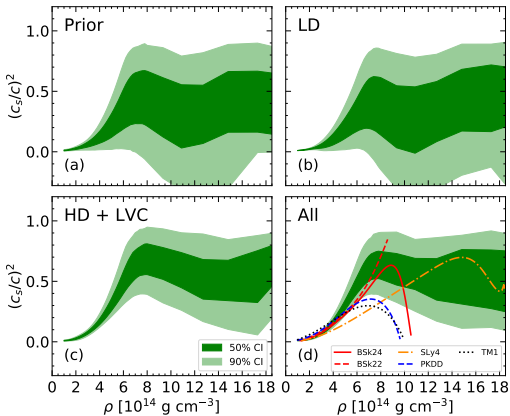
Miller et al 2021, arXiv:2105.06979 .

Backup slides 2: Some extra results

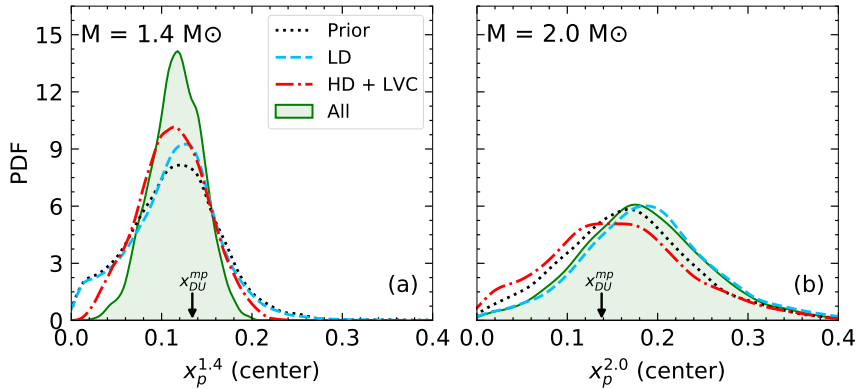
1. NM energy



2. Sound speed



3. Proton fraction



4. Correlation among observables

n_{CC}																			
P_{CC}	0.88																		
$R_{crust}^{1.4}$	0.52	0.61																	
$R_{1.4}$	-0.17	-0.23	0.62	$\Lambda_{1.4}$	$x_p^{1.4}$	$R_{crust}^{2.0}$	$R_{2.0}$	$\Lambda_{2.0}$	$x_p^{2.0}$										
$\Lambda_{1.4}$	-0.03	-0.14	0.65	0.97	$x_p^{1.4}$	-0.20	-0.23	0.14	0.40	0.31									
$x_p^{1.4}$	-0.20	-0.23	0.14	0.40	0.31	$R_{crust}^{2.0}$	0.49	0.55	0.93	0.61	0.68	-0.08							
$R_{2.0}$	0.01	-0.04	0.66	0.88	0.92	$R_{2.0}$	0.06	0.81	$\Lambda_{2.0}$	0.10	0.03	0.65	0.81						
$\Lambda_{2.0}$	0.10	0.03	0.65	0.81	0.88	$\Lambda_{2.0}$	-0.05	0.83	0.98	$x_p^{2.0}$	-0.02	-0.07	0.14	0.25	0.22	0.89	-0.08	-0.05	-0.12
$x_p^{2.0}$	-0.02	-0.07	0.14	0.25	0.22	$x_p^{2.0}$	-0.08	-0.05	-0.12	n_{CC}	P_{CC}	$R_{crust}^{1.4}$	$R_{1.4}$	$\Lambda_{1.4}$	$x_p^{1.4}$	$R_{crust}^{2.0}$	$R_{2.0}$	$\Lambda_{2.0}$	

5. Correlation among parameters

